OBSERVATION OF LASER-BEAM BENDING DUE TO TRANSVERSE PLASMA FLOW

P. E. Young *E. A. Williams*

C. H. Still *R. L. Berger*

D. E. Hinkel *K. G. Estabrook*

W. L. Kruer

Introduction

The propagation of intense laser pulses through fully ionized plasmas can be affected by a number of processes that can be linear, such as refraction due to transverse density gradients, or nonlinear in the case of the filamentation instability. While laser-beam propagation in the direction normal to the density gradient and plasma flow have been studied thoroughly, transverse flow introduces new considerations and can, for example, influence the growth rate of filamentation [1]. This is an important consideration for hohlraum targets used in inertial confinement fusion applications where plasma flowing across the beam near the entrance hole can steer the beam. As a result, the symmetry of the intended x-ray drive can change because the position of the laser spot on the hohlraum wall is moved. Transverse flow steers the beam when the laser is sufficiently intense that the ponderomotive force causes the plasma to pile up against the beam, which produces a density gradient that refracts the beam towards the downstream direction. This effect is particularly strong when the transverse flow velocity equals the sound speed of the plasma.[1,2] Although some evidence of this effect has recently been reported,[3] quantitative comparison to theoretical predictions requires a well characterized background plasma and knowledge of the laser beam path through the plasma.

In this article, we describe the results of an experiment in which we interferometrically observe the density channel produced by an intense laser beam propagating through a preformed plasma. We observe beam bending in the presence of transverse plasma flow that increases as the laser intensity is increased, which rules out refractive effects due to the unperturbed density profile. An important point is that the beam bending occurs at a very low density ($\sim 0.05 n_c$) where the filamentation threshold is not exceeded. For a laser intensity of 1.5×10^{15} W/cm^2, we observe beam deflections of 10 degrees, which is in quantitative agreement with the calculations of the F3D hydrodynamic code.[4] The code uses the experimentally measured density and flow velocity profiles and a laser electric field reconstructed from the measured near-field phase profile of the experimental laser beam.

Some simple estimates illustrate the physics of beam bending. Consider a beam propagating through a flowing plasma with electron density n_e. Its ponderomotive pressure creates a density depression of magnitude $\Delta n / n \approx (v_o / v_e)^2 / (1 - M^2)$, where v_o is the electron quiver velocity in the laser field, v_e is the electron thermal velocity, and M is the Mach number of the flow component transverse to the direction of propagation. The density perturbation is swept downstream of the intensity maximum so that the light sees a refracting gradient $\nabla_\perp \Delta n \sim (n_e / L_T)(v_o / v_e)^2 (1 - M^2)^{-1}$, where L_T is the characteristic transverse dimension of the laser beam. The light is deflected by ray optics through an angle, θ, given by

$$\theta \approx (1/2n_c)\int \nabla_\perp \Delta n \, dz$$
$$= (1/2)(n_e / n_c)(v_o / v_e)^2 L_T^{-1} \int dz \, [1 - M(z)^2]^{-1}. \quad (1)$$

As $M \Rightarrow 1$, the simple linear estimate for Δn, above, fails. Within some range, ΔM of the sonic point at M = 1, the density perturbation saturates, either nonlinearly ($\Delta M \sim v_o / v_e$) (Ref. 5) or from finite ion acoustic damping ($\Delta M \sim \nu_{ia} / \omega_{ia}$, where ν_{ia} / ω_{ia} is the ion acoustic damping decrement).[6,7]

Independent of the saturation mechanism and of the magnitude of ΔM ($<< 1$), we can estimate the integral in Eq. 1 by $L_v / 2$, where L_v is the scalelength of the transverse velocity variation at the sonic point, giving

$$\theta \approx (1/4)\,(n_e / n_c)(v_o / v_e)^2 (L_v / L_T). \quad (2)$$

For a beam with internal structure, L_T can be expected to be characteristic of the typical hot spot

dimensions, ~$f\lambda$, rather than the total beam width. In this experiment, the beam phase was measured, making quantitative comparison with numerical calculation well motivated.

Note that the mechanism for beam bending is independent of filamentation. With increasing intensity, however, existing hot spots in the laser beam will be intensified by self-focusing. One anticipates from Eq. 2 that the increasing intensity and reduced lateral dimension of self-focused hot spots should increase beam bending. Strong filamentation, however, can be expected to cause beam breakup and the lack of identifiable channels.

An important point is that in this experiment, the observed beam bending occurs at a very low density before filamentation can occur, so filamentation is decoupled from the beam bending process. Filamentation results in the spraying of the beam and produces the termination of the channel near the peak of the plasma density, as observed by the interferometer. The imaginary wave number for ponderomotive filamentation is given by:[8]

$$k_I = (k_R / 2k_0)\,(1/2)[(\omega_0{}^2 / c^2)(n_e / n_c)\,(v_0 / v_e)^2 - k_R{}^2]^{1/2}, \quad (3)$$

where k_R is the transverse size of the filaments. Since the beam width is only 20 μm, the filaments must be less than 10 μm in size to grow. For exponential growth, $2k_I L \cong 1$. For the conditions $k_R / k_0 = 5$, $n / n_c = 0.05$, $T_{keV} = 0.5$, $L_\mu = 50$, and $\lambda_\mu = 1.064$, we find that $I_p = 4.5 \times 10^{15}$ W/cm^2 is required for exponential growth, which is three times the vacuum intensity. This analysis neglects the lowering of the background density in the beam channel, which would further raise the threshold intensity. In fact, both the experiments and the simulations show a well-defined channel all the way to the peak of the density profile (~$0.3n_c$), indicating that filamentation is not important at the lower densities.

Experimental Description

The present experiment was conducted using the Janus laser at Lawrence Livermore National Laboratory where we have developed a test bed for studying the propagation of moderately intense laser pulses through well-characterized underdense plasmas.[9] A 1.064-μm wavelength, 100-ps full-width at half-maximum (FWHM) Gaussian pulse interacted with an underdense plasma formed by the irradiation of a 0.35-μm-thick parylene [$(CH)_n$] foil by a 1-ns, 0.532-μm wavelength, 400-μm-diam, 2×10^{13} W/cm^2 laser pulse. Both a line focus and a circular focus were used for the interaction beam at various points in the experiment. A line focus (20 μm × 400 μm, peak intensity = 1.5×10^{15} W/cm^2) was used because the long path length through the channel makes the observed phase change due to the density depression easy to see.[10] To observe the behavior of the channel at higher intensities, we used a circular focus to achieve a peak intensity of 5×10^{16} W/cm^2. The best focus of the interaction beam in all cases is located at the target plane, and its vacuum properties[10] are constant as the laser intensity is varied by changing the amplifier gain, which changes the laser energy. Varying the relative timing between the plasma formation and interaction pulses (1.5- to 2.5-ns delay from the end of the plasma-forming pulse) determined the peak density (0.25 to $0.1n_c$) seen by the interaction pulse. The background density profile was measured using a folded-wave interferometer. The 50-ps, 0.35-μm wavelength interferometer probe pulse arrived at the target at the same time as the peak of the 100-ps interaction pulse.

To introduce a component of the plasma flow that is transverse to the propagation direction of the interaction beam, the target foils are tilted at angles up to 45 degrees. Since the plasma flow is normal to the target surface, the target angle determines the transverse flow velocity seen by the interaction pulse.

Results and Analysis

The main experimental results are summarized in Figure 1. At the highest intensity (for a line focus), we see obvious beam bending (~10 degrees) at the outer edge of the plasma where the density is low (~$0.05n_c$), but the flow velocity is high (~1×10^8 cm/s) compared to the sound speed, c_s (~3×10^7 cm/s). The bending is localized, and the channel stays well-defined up to the peak plasma density (~$0.3n_c$), after which it disappears; this is because of beam breakup and spreading due to filamentation.[10,11]

As we vary the incident laser intensity, the amount of bending becomes substantially less (see Figure 1) until there is a 1 degree deflection for an intensity of 2×10^{14} W/cm^2, clearly showing that this is an intensity-dependent effect and not due to linear refraction in the inhomogeneous plasma distribution. We observe a similar reduction in bending angle as we decrease the target angle, as expected.

The deflection predicted by the simple analytic model of Eq. 2 agrees well with that observed in the experiment. For the line focus, we take $n / n_c \cong 0.05$, $I = 1 \times 10^{15}$ W/cm^2, $T_e = 500$ eV, $L_v \cong 200$ μm, and $L_T \cong 10$ μm, and find $\theta \cong 13^o$, close to what is observed in the experiment. Of course, quantitative calculations need to account for detailed beam structure, laser-beam filamentation, and various 3D effects. For example, when a circular focus is used to obtain a very high intensity (5×10^{16} W/cm^2), no beam deflection is detected. This result is in agreement with the nonlinear model of Rose,[6,12] who has discussed a regime in which the plasma can simply flow around a small beam, an effect which clearly decreases the deflection.

We will next show experimentally that the location of the beam bending occurs where the transverse flow

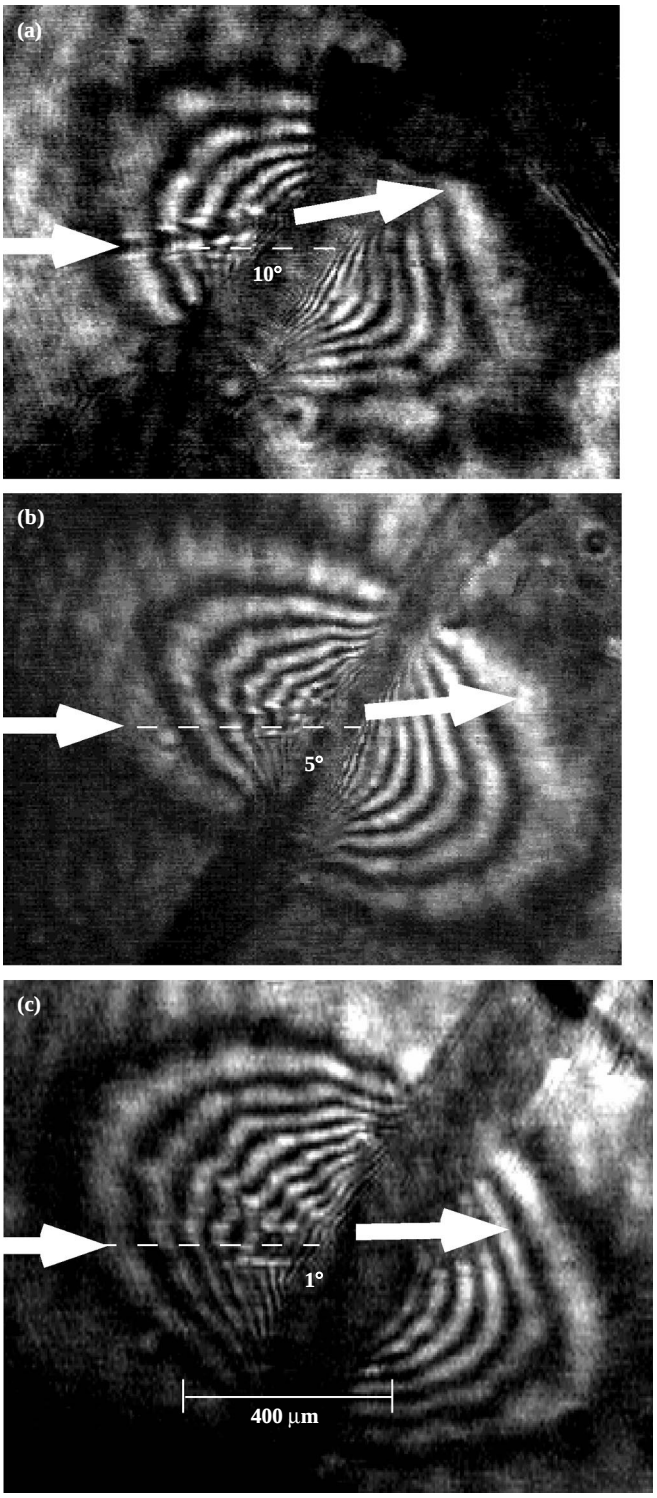

FIGURE 1. Interferograms that show variation in channel bending for peak laser intensities of (a) 1.5×10^{15}, (b) 1×10^{15}, and (c) 5×10^{14} W / cm^2. (50-00-0598-1155pb01)

velocity equals the inferred sound speed c_s. We do this by obtaining plasma interferograms at different times (100-ps steps) relative to the end of the plasma-forming pulse on sequential irradiations of the target. We then Abel invert the interferograms to obtain the plasma density distribution. By using the continuity equation, $\partial n_e / \partial t = \nabla \bullet (n_e \mathbf{v})$, where $\mathbf{v}$ is the flow velocity, we can recover the velocity distribution of the plasma, using the boundary condition, $v = 0$, at the peak of the density profile. We also assume that $\mathbf{v}$ is parallel to ∇n_e. Test calculations with 1D analytic expansion profiles and 2D LASNEX hydrodynamic simulations show that our calculations underestimate the flow velocity at the outer edge of the plasma by ~20%, mainly due to the approximation of calculating dn / dt from the difference of two plasma profiles separated by 100 ps. The outer edge expansion can be corrected, however, by measuring the propagation speed of the outermost fringe in the interferograms. The results are shown in Figure 2 for the conditions of Figure 1; we find a transverse flow velocity of 2×10^7 cm / s, which is close to both the sound speed inferred from earlier Thomson scattering measurements (T_e = 700 eV) on solid carbon targets[13] and the prediction of 2D LASNEX simulations (T_e = 300 eV).

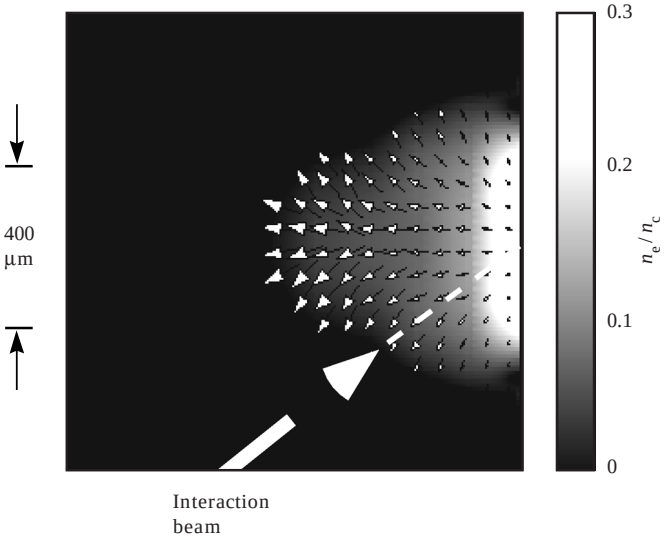

FIGURE 2. Density and flow velocity distributions calculated from the experimental data. The longest arrow corresponds to a flow velocity of 1.4×10^8 cm / sec. (50-00-0598-1156pb01)

Comparison to Numerical Simulations

To understand the laser propagation behavior, the experimental results are compared to numerical simulations. Such simulations will be used predict the performance of NIF-scale targets, so it is important to have a detailed experimental benchmark for the code. To model the experiment, we used a version of the F3D code[4] that incorporated a fully 3D nonlinear Eulerian hydrodynamics package (NH3) in Cartesian

coordinates. F3D is a fully nonlinear, time-dependent code in which the hydrodynamic and heat transport are coupled to the light wave propagation.

The experiment was duplicated in the simulation as much as possible. We modeled the electric field and phase distributions of the interaction beam by using an input phase profile that was experimentally measured using radial shear interferometry and numerically propagating the beam through the lenses used in the experiment (aspheric lens, 20-cm focal length, and two 3.94-m focal length cylindrical lenses that were crossed at a 45° angle to produce the appropriate line focus length). The calculated intensity distribution agrees well with equivalent plane images that were obtained from the experiment (see Figure 3).

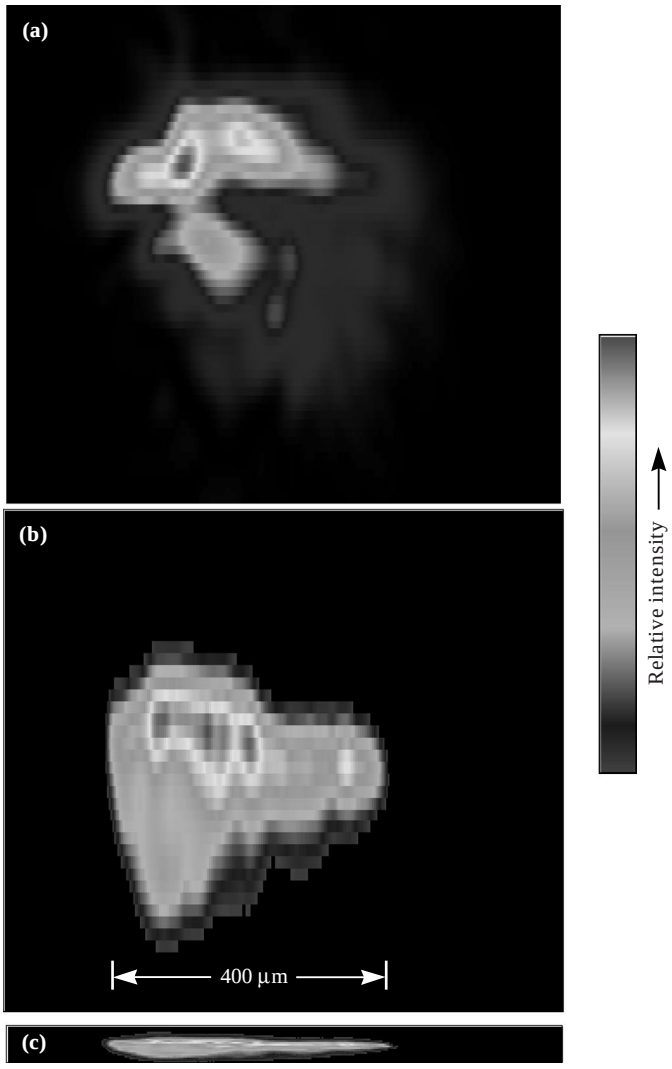

FIGURE 3. Comparison of (a) the calculated intensity using the measured near-field phase-front profile, and (b) the equivalent target plane image of the line focus. The vertical scales of (a) and (b) have been expanded (box heights are 40 μm versus 500 μm for the width of the boxes) to facilitate comparison of the detailed intensity structure. The measured spot in normal aspect ratio is shown in (c). (50-00-0598-1157pb01)

The measured density and flow velocity profiles were used as the starting conditions for the simulation. The 100-ps Gaussian pulse shape used in the experiment is modeled in the simulations by a smoothly rising ramp, $S(t) = 1 - [1 - (t/tp)^2]^2$, where t_p = 100 ps. The measured electron density and flow velocity profiles were used as the initial conditions for the simulation. Because of the narrow cross section of the laser beam, it is only necessary to model a region with transverse dimension of 120 μm and axial dimension of 350 μm. Over this transverse scale, the density and flow can be taken as uniform along the transverse direction initially, but both vary along the axial laser propagation direction. Even after the beam deflects at low density and filaments at higher density, the beam stayed away from the simulation edges as shown in the example in Figure 4. The electron temperature is initially uniform with values taken between 300 and 700 eV to bracket the LASNEX predictions and the Thomson scattering measurements; best agreement with the experiment is found for T_e = 500 eV. The ponderomotive force acts locally to modify the density with nearly 100% modulation at the higher density where the beam breaks up.

Figure 4 shows the calculated density channels, averaged over 50 ps, centered on the peak of the laser pulse, that are formed in the background density profile. The calculations with the experimental flow profile (see Figure 4a) clearly shows a bend of about 10 degrees, in agreement with the experiment. No deflection occurs if the transverse flow is intentionally turned off (see Figure 4b). The initial bend is at the sonic point for an initial temperature of 500 eV. The channel persists for 200 μm past the sonic point, in good agreement with the

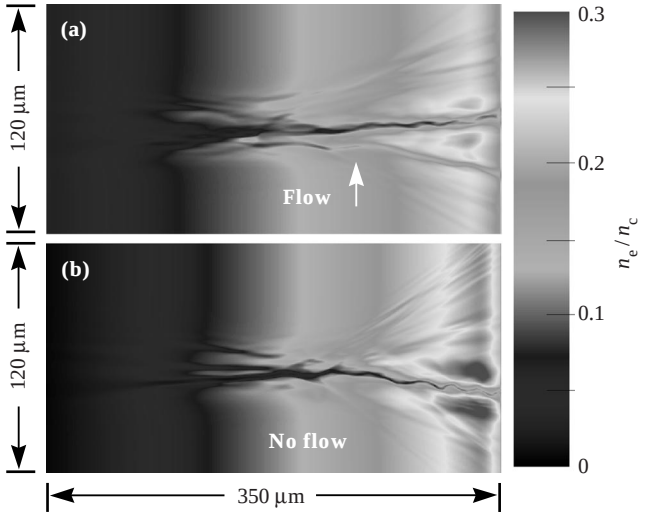

FIGURE 4. Density distributions calculated by F3D using the experimental density profile (a) with the experiment flow velocity profile and (b) with no plasma flow. The simulation has been averaged over 50 ps centered on the peak of the pulse. The laser enters from the left side of the box and propagates to the right. (50-00-0598-1158pb01)

experiment. We performed a number of simulations at different intensities bracketing the nominal laser intensity of the interaction beam. When the simulation intensity is increased by a factor of 5 or greater, the beam breaks up near focus, leaving no clearly defined density channel readily observable by interferometry. Decreasing the simulation intensity results in a decrease in the deflection angle, as expected, with no deflection observed when the intensity is a factor of 100 smaller than the nominal intensity. The scaling of the deflection angle with the laser intensity is in rough agreement with the prediction of Eq. 2.

Conclusion

We have quantitatively measured the beam deflection in a plasma due to transverse plasma flow. The deflection at moderate intensities is predicted well by a simple analytic model. A nonlinear hydrodynamic model using the experimental laser-beam electric field profile, plasma density, and flow velocity distributions shows excellent agreement with the experiment.

Acknowledgments

We thank W. Seka for valuable discussions concerning the near-field phase-front measurement of the laser beam. We would like to thank J. Hunter, G. London, B. Sellick, and J. Foy for technical assistance during the experiment.

Notes and References

1. R. W. Short, R. Bingham, and E. A. Williams, *Phys. Fluids* **25**, 2302 (1982).
2. D. E. Hinkel, E. A. Williams, and C. H. Still, *Phys. Rev. Lett.* **77**, 1298 (1996).
3. J. D. Moody et al., *Phys. Rev. Lett.* **77**, 1294 (1996).
4. R. L. Berger et al., *Phys. Fluids B* **5**, 2243 (1993).
5. W. L. Kruer and J. H. Hammer, *Comments Plasma Phys. Cont. Fusion* **18**, 85 (1997).
6. H. A. Rose, *Phys. Plasmas* **3**, 1709 (1996).
7. D. E. Hinkel et al., *Phys. Plasmas* (in press).
8. W. L. Kruer, *Comments Plasma Phys. Controlled Fusion* **9**, 63 (1985).
9. P. E. Young, M. E. Foord, J. H. Hammer, W. L. Kruer, M. Tabak, and S. C. Wilks, *Phys. Rev. Lett.* **75**, 1082 (1995).
10. P. E. Young, J. H. Hammer, S. C. Wilks, and W. L. Kruer, *Phys. Plasmas* **2**, 2825 (1995).
11. S. C. Wilks, P. E. Young, J. Hammer, M. Tabak, and W.L. Kruer *Phys. Rev. Lett.* **73**, 2994 (1994).
12. S. Ghosal and H. A. Rose, *Phys. Plasmas* **4**, 2376 (1997).
13. P. E. Young, *Phys. Rev. Lett.* **73**, 1939 (1994).